Optimum Nonseparable Filter Bank Design in Multidimensional M-Band Subband Structure

Kyusik Park*, Woncheol Lee**

ABSTRACT

A rigorous theory for modeling, analysis, optimum nonseparable filter bank in multidimensional M-band quantized subband codec are developed in this paper. Each pdf-optimized quantizer is modeled by a nonlinear gain-plus-additive uncorrelated noise and embedded into the subband structure. We then decompose the analysis/synthesis filter banks into their polyphase components and shift the down-and up-samplers to the right and left of the analysis/synthesis polyphase matrices respectively. Focusing on the slow clock rate signal between the samplers, we derive the exact expression for the output mean square quantization error by using spatial-invariant analysis. We show that this error can be represented by two uncorrelated components : a distortion component due to the quantizer gain, and a random noise component due to fictitious uncorrelated noise at the quantizer. This mean square error is then minimized subject to perfect reconstruction (PR) constraints and the total bit allocation for the entire filter bank. The algorithm gives optimum filter coefficients and subband bit allocations. Numerical design example for the optimum nonseparable orthonormal filter bank is given with a quincunx subsampling lattice.

I. INTRODUCTION

Subband coding has been proposed for many applications in the field of speech, image, and video compression. Presently the DCT is the industry standard; however future application such as MPEG-4 may require greater compression and performance than that obtained from the block transform coding.

In the absence of quantization noise, prefect reconstruction(PR) theory for multidimensional subband filter bank(FB) is well established[1]-[5]. The multidimensional multirate FB is not a simple extension of the one-dimensional(1-D) FB except for the separable case. The main complication arises from the subsampling lattice D in the decimator[1][6]. In 1-D, the downsampler retains every Mth sample in the sequence, discards the rest, and then reindexes the time scale. In multiple-dimension, the decimator retains samples located on a subsampling lattice, which is represented by the subsampling matrix D, with integer elements. Thus the filter design problem necessarily depends on the choice of sampling matrix. For the separable FB with a diagonal matrix D, most of the results from 1-D FB can be easily extended to the multiple dimension in a separable fashion along each dimension[5]. However, the nonseparable case, is far more complex and the effect of sampling matrix D must be carefully considered into the design problem.

Most of the previous works in multidimension have been developed under the assumption of no quantization noise and of simple separability conditions of the filter bank. Woods and O'Neil[3] have introduced 16 bands separable filter bank system to code pictures with DPCM. But they used existing quadrature mirror filter(QMF) to split the subband images. Westerink, et al[7] also decomposed the image into 16 separable subbands, but encoded with a vector quantization. In ref. [8], they also showed the analysis of a two band quantized FB structure and used a QMF on the actual test image in a deterministic way. Vandendorpe[9] assigned some subjective weights to different frequency bands and minimized the weighted quantization noise. But he assumed a simple input-independent white additive quantization noise model which is not valid for the pdf-optimized quantizer[10]. Yet neither the actual mathematical analysis of the quantization noise nor the optimum nonseparable filter bank design with quantization errors embedded explicitly in the criterion have been reported in multidimensional filter bank so far.

This paper is an extension of the one-dimensional work in [11] to multiple-dimensions. A key approach is the

* Department of Information and Telecommunication, Sangmyung University
** Department of Information and Telecommunication, Engineering, Sungsil University

Manuscript Received April 22, 1996.

model-based decorrelation of the quantization noise from the input signal by use of the gain-plus-additive noise model for the pdf-optimized quantizer. We then embed the quantizer noise model into the subband structure. Using polyphase decomposition of the FBs, we calculate the output MS quantization error as the sum of two components; a distortion and a random component. This mean square error(MSE) serves as the measure in the design and evaluation of quantized subband filter banks.

This paper outline is as follows: Section II provides a brief review of the quantization model and the basic notations and definitions in multidimensional multirate FB theory. In Section III, we develop the optimum multidimensional M-band filter bank structure in the presence of pdf-optimized quantizers as a generalization of 1-D filter bank theory presented in [11]. We derive the multidimensional version of MS quantization error formula at the reconstructed output by using the polyphase decomposition of the filter bank. As we will see, the derivation is quite straightforward, but the underlying theory is quite different from the 1-D case. Section IV describes the optimum filter design methodology in multidimensional subband structures. Specific design example for the nonseparable orthonormal FB with quincunx sampling matrix is investigated.

II. PRELIMINARIES

In this section, we first review the gain-plus-additive noise model for the pdf-optimized quantizer advanced by Jayant & Noll. Then we briefly summarize the basic notations and definitions in multidimensional multirate filter bank theory that will be used throughout this paper.

A. Quantization Model

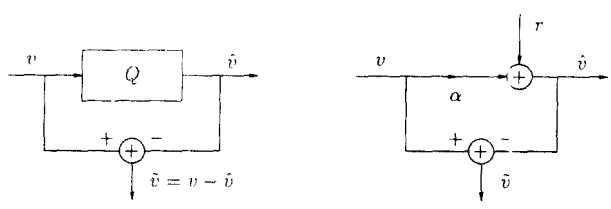

Fig. 1 (a) Pdf-optimized quantizer, (b) gain-plus-additive noise model.

Fig. 1(a) shows the block diagram representation of the pdf-optimized quantizer: v, the signal to be quantized, is a input random variable with a known pdf $p_v(v)$ with zero mean and variance σ_v^2; $\hat{v}$ is the quantized output; and $\tilde{v}$ is the quantization error with variance

$$\sigma_{\tilde{v}}^2 = \int_{-\infty}^{+\infty} \tilde{v}^2 p_{\tilde{v}}(\tilde{v})\, d\tilde{v} = \int_{-\infty}^{+\infty} (v-\hat{v})^2 p_v(v)\, dv \tag{1}$$

The quantizer that minimizes this MSE is called the pdf-optimized Lloyd-Max quantizer[12][13].

For the pdf-optimized quantizer, it can be shown that the quantization error is unbiased and that the error is orthogonal to the quantizer output[6][10]

$$E[\tilde{v}] = 0, \qquad E[\hat{v}\tilde{v}] = 0. \tag{2}$$

This implies quantization error $\tilde{v}$ is correlated with the input v, and that the variance of $\tilde{v}$

$$\sigma_{\tilde{v}}^2 = \sigma_v^2 - \sigma_{\hat{v}}^2. \tag{3}$$

Hence, the input-independent-additive noise model is only a approximation to the pdf-optimized quantizer.

Fig. 1(b) shows a gain-plus-additive noise model representation which is to model the quantizer. As suggested by Jayant & Noll[10], we can choose the input signal-dependent gain α and the variance of random fictitious noise r as

$$\alpha = 1 - \frac{\sigma_{\tilde{v}}^2}{\sigma_v^2}, \quad \sigma_r^2 = \alpha(1-\alpha)\sigma_v^2 = \alpha\sigma_{\tilde{v}}^2. \tag{4}$$

Then this choice force r and v to be uncorrelated such that

$$E[r\,v] = E[v - \alpha v - \tilde{v})\,v] = (1-\alpha)\sigma_v^2 - \sigma_{\tilde{v}}^2 = 0, \tag{5}$$

further it satisfies the conditions in (2).

B. Review of Notations and Definitions in Multidimensional Filter Bank [1][6]

Let the N-dimensional discrete signal $x(\underline{n})$ be defined on an integer lattice Λ, where $\underline{n} = (n_1, n_2, \cdots, n_N)^T$ is the set of all integer vectors. With the transform variables and integer matrix D

$$\underline{z} = [z_1, z_2, \cdots, z_N]^T,$$
$$\underline{w} = [w_1, w_2, \cdots, w_N]^T,$$

$$D = [d_1, d_2, \cdots, d_N] = \begin{bmatrix} d_{11} & d_{12} & \cdots & d_{1N} \\ d_{21} & d_{22} & \cdots & d_{2N} \\ \vdots & \vdots & \ddots & \vdots \\ d_{N1} & d_{N2} & \cdots & d_{NN} \end{bmatrix}, \tag{6}$$

we define

$$\underline{z}^{\underline{n}} = \Pi_{k=1}^{N} z_k^{n_k},$$

$$\underline{z}^{D} = \begin{bmatrix} \underline{z}^{\underline{d}_1} \\ \underline{z}^{\underline{d}_2} \\ \vdots \\ \underline{z}^{\underline{d}_n} \end{bmatrix} = \begin{bmatrix} z^{d_{11}} & z^{d_{12}} & \cdots & z^{d_{1n}} \\ z^{d_{21}} & z^{d_{22}} & \cdots & z^{d_{2n}} \\ & & \vdots & \\ z^{d_{n1}} & z^{d_{n2}} & \cdots & z^{d_{nn}} \end{bmatrix}, \tag{7}$$

Then the Z and Fourier transform of the discrete N-dimensional signal $x(\underline{n})$ can be written as

$$X(\underline{z}) = \sum_{\underline{n} \in \Lambda} x(\underline{n}) z^{-\underline{n}}, \leftrightarrow X(e^{j\underline{w}}) = \sum_{\underline{n} \in \Lambda} x(\underline{n}) e^{j\underline{w}^T \underline{n}}. \tag{8}$$

Let Λ_D be a sampling sublattice which is the set of all integer vectors $\underline{m} = (m_1, m_2, \cdots, m_N)^T$ generated by $\underline{m} = D\underline{n}$ of the nonsingular integer sampling matrix D for some integer vectors $\underline{n}$. A given sublattice Λ_D can be described by more than one sampling matrix and the sampling matrices are related to each other by postmultiplication by an integer matrix with determinant equal to ± 1. For example, the following two-dimensional quincunx sampling matrices[4][5]

$$D_1 = \begin{bmatrix} 1 & 1 \\ 1 & -1 \end{bmatrix}, \qquad D_2 = \begin{bmatrix} 1 & -1 \\ 1 & 1 \end{bmatrix} \tag{9}$$

define the same sublattice as in Fig. 2.

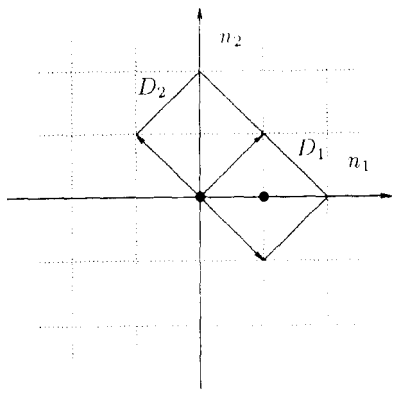

Fig. 2 Sublattice defined by D_1, D_2(• : coset vectors associated with D_1).

The coset is the set of points obtained by shifting the origin of sublattice Λ_D defined by sampling matrix D by integer vectors $\underline{k}$ in the unit cell. The integer shift vectors $\underline{k}$ are called the coset vectors associated with D and there are exactly $M = |\det D|$ of distinct coset vectors denoted by $\{\underline{k}_0, \underline{k}_1, \cdots, \underline{k}_{M-1}\}$. For example, with the quincunx sampling matrix D_1 in (9), the associated coset vectors are

$$\underline{k}_0 = \begin{pmatrix} 0 \\ 0 \end{pmatrix}, \qquad \underline{k}_1 = \begin{pmatrix} 1 \\ 0 \end{pmatrix} \tag{10}$$

shown(•) in Fig. 2. Clearly, the union of two cosets associated with above coset vectors for a given sublattice yields the rectangular lattice.

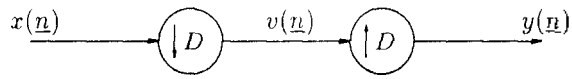

Fig. 3 Representation of N-dimensional down-and up-sampling.

The sampling operations in multidimensional filter banks is represented diagramatically in Fig. 3 and defined by

$$v(n) = x(Dn), \; y(\underline{n}) = \begin{cases} v(D^{-1}\underline{n}) & D^{-1}\underline{n} \text{ an integer vector} \\ 0, & \text{otherwise} \end{cases} \tag{11}$$

so that

$$y(\underline{n}) = \begin{cases} x(n), & \underline{n} \in \Lambda_D \\ 0, & \text{otherwise} \end{cases} \tag{12}$$

The downsampler accepts samples lying on the sublattice Λ_D, discards others, and reindexes the spatial axes. The z-transform is given by

$$V(\underline{z}) = \frac{1}{M} \sum_{l=0}^{M-1} X(\underline{z}^{D^{-T}} e^{-j2\pi D^{-T} \underline{k}_l}) \tag{13}$$

where D^{-T} is transpose of D^{-1} and $M = |det\, D|$. The upsampler takes points $v(\underline{n})$ on a rectangular lattice and maps them into the sublattice Λ_D and the z-transform is

$$Y(z) = V(\underline{z}^D). \tag{14}$$

Thus the combined operation from input to output yields

$$Y(z) = \frac{1}{M} \sum_{l=0}^{M-1} X(\underline{z}\, e^{-j2\pi D^{-1} \underline{k}_l}), \tag{15}$$

and the output is simply those input points that lie on the sublattice Λ_D.

Throughout the rest of this paper, we will heavily rely on the notations and definitions from [1][6].

III. Quantization Error Analysis in Nonseparable N-dimensional M-Band Subband Structure

The nonseparable N-dimensional M-band FB with pdf-

optimized quantizers is shown in Fig. 4(a). The structure is maximally decimated (or critically sampled) if the number of channels is equal to $M=|\det D|$ and we will only consider this case.

By using polyphase decomposition of the analysis/synthesis filter bank, we can show that

$$\mathcal{H}_k(\underline{z})=\sum_{l=0}^{M-1} \underline{z}^{-\underline{k}_l}\mathcal{H}_{k,l}(\underline{z}^D) \leftrightarrow \mathcal{H}_{k,l}(\underline{z})=\sum_{\underline{n}\in\Lambda} h_k(D\underline{n}+\underline{k}_l)\underline{z}^{-\underline{n}},$$

$$\mathcal{G}_k(\underline{z})=\sum_{l=0}^{M-1} \underline{z}^{\underline{k}_l}\mathcal{G}_{k,l}(\underline{z}^D) \leftrightarrow \mathcal{G}_{k,l}(\underline{z})=\sum_{\underline{n}\in\Lambda} g_k(D\underline{n}+\underline{k}_l)\underline{z}^{-\underline{n}} \tag{16}$$

for $k=0, 1, \cdots, M-1$. Note that the positive exponent shift vectors are used at the synthesis side to compensate for the delays at the analysis side. We can also note the difference in forming the polyphase component of the analysis/synthesis filters between the 1-dimension and the N-dimension filter bank. In 1-D, the coset vectors are the points on the interval $[0, M-1]$ defined by the scalar factor M. To get the analysis polyphase component, we shift $h_k(n)$ by l and subsample the translated $h_k(n+l)$ by M to get $h_k(Mn+l)$ for each $l\in[0, M-1]$. On the other hand, to obtain the N-dimensional analysis polyphase expansion, we select the N-dimensional coset vectors $\{\underline{k}_0, \underline{k}_1, \cdots, \underline{k}_{M-1}\}$ associated with $N\times N$ sampling matrix D and shift $h_k(n)$ by $\underline{k}_l$ and downsample by D to get $h_k(Dn+\underline{k}_l)$. We can aslo make the same arguement about the synthesis polyphase components.

Then the analysis/synthesis filter bank can be represented in terms of the polyphase matrices $\mathcal{H}_p(z)$ and $\mathcal{G}_p^T(\underline{z})$

$$\mathcal{H}_p(\underline{z})=[\mathcal{H}_{p,k}(\underline{z})]_{M\times M}, \quad \mathcal{G}_p(\underline{z})=[\mathcal{G}_{p,k}(\underline{z})]_{M\times M} \tag{17}$$

in the same manner as in the 1-D case[11], but with a vector notation. We then replace the bank of pdf-optimized quantizers by gain-plus-additive noise model, and the analysis and synthesis filter banks by their polyphase equivalents in Fig. 4(b). In this case, the transpose of $\mathcal{G}_p(z)$ emerges as the synthesis polyphase matrix followed by positive exponent shift vectors. Now the system is spatially-invariant

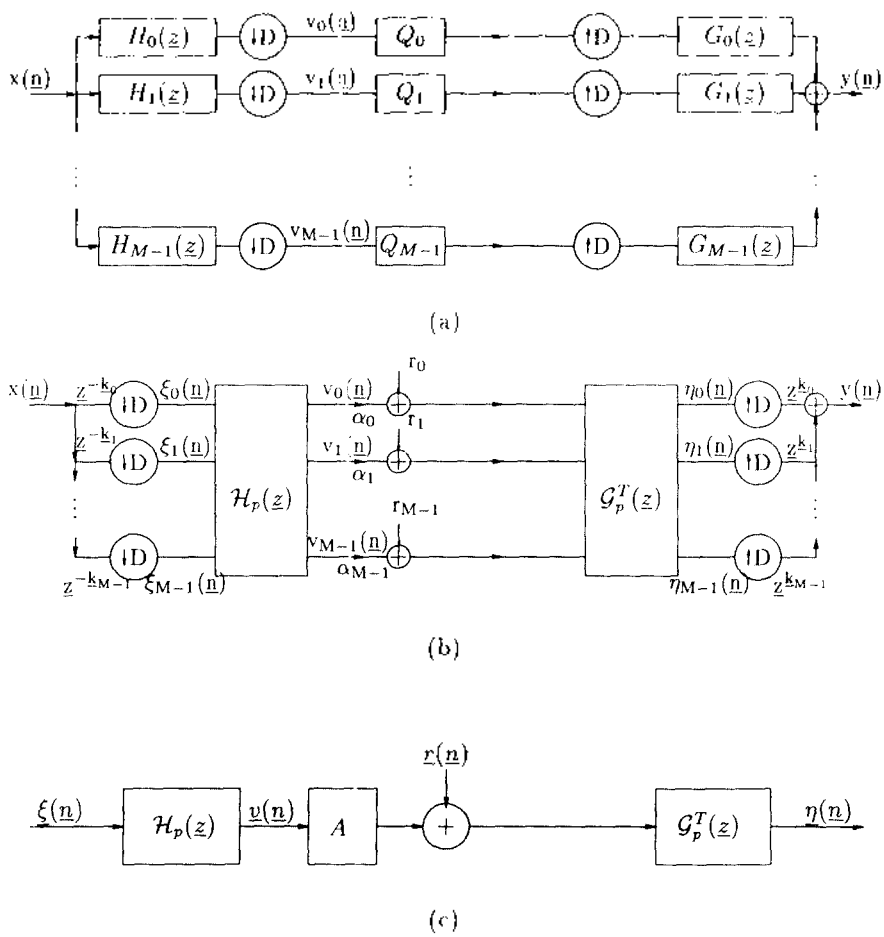

Fig. 4 (a) Multidimensional nonseparable M-band FB with quantizers, (b) polyphase equivalent structure, (c) equivalent vector-matrix representation.

from $\xi(\underline{n})$ to $\eta(\underline{n})$ and can be represented by Fig. 4(c). In this figure, A is diagonal gain matrix such that

$$A = \mathrm{diag}[\alpha_0, \alpha_1, \cdots, \alpha_{M-1}],$$
$$S = \mathrm{diag}[s_0, s_1, \cdots, s_{M-1}] \tag{18}$$

where $\alpha_i = 1 - \sigma_{\hat{v}_i}^2 / \sigma_{v_i}^2$ and $\sigma_{\hat{v}_i}^2 = \beta_i 2^{-2R_i} \sigma_{v_i}^2$ for $i = 0, 1, \cdots, M-1$.

From Fig. 4(c), the total quantization error $\underline{\eta}_q(\underline{z})$ is the difference

$$\begin{aligned}\underline{\eta}_q(\underline{z}) &= \underline{\eta}_q(\underline{z}) - \underline{\eta}_o(z) \\ &= \mathcal{G}_p^T(\underline{z})(A - I)\mathcal{H}_p(\underline{z})\underline{\xi}(\underline{z}) + \mathcal{G}_p^T(\underline{z})\underline{R}(\underline{z})\end{aligned} \tag{19}$$

where I is $M \times M$ identity matrix and $\underline{\eta}_o(\underline{z})$ is the system output without quantizers.

For notational convenience, we define $M \times M$ diagonal matrix

$$B \triangleq A - I = \mathrm{diag}[\alpha_0 - 1, \alpha_1 - 1, \cdots, \alpha_{M-1}], \tag{20}$$

and substitute decimated signal $\underline{V}(\underline{z}) = \mathcal{H}_p(\underline{z})\underline{\xi}(\underline{z})$ into (19) to obtain

$$\begin{aligned}\underline{\eta}_q(\underline{z}) &= \mathcal{G}_p^T(\underline{z})B\underline{V}(\underline{z}) + \mathcal{G}_p^T(\underline{z})\underline{R}(\underline{z}) \\ &= \underline{\eta}_d(\underline{z}) + \underline{\eta}_n(\underline{z})\end{aligned} \tag{21}$$

where $\underline{\eta}_d(\underline{z})$ is a signal distortion component due to the quantizer gains and $\underline{\eta}_n(\underline{z})$ is a random component due to the random fictitious noise.

Since $\underline{v}(\underline{n})$ and $\underline{r}(\underline{n})$ are uncorrelated from the quantizer model, we can derive the output power spectral density (PSD) of the quantization error $\underline{\eta}_q(\underline{z})$

$$S_{\underline{\eta}_q\underline{\eta}_q}(\underline{z}) = \mathcal{G}_p^T(-\underline{z}^{-1})BS_{\underline{v}\underline{v}}(\underline{z})B(\mathcal{G}_p^T(\underline{z}))^T + \mathcal{G}_p^T(-\underline{z}^{-1})S_{\underline{r}\underline{r}}(\underline{z})(\mathcal{G}_p^T(\underline{z}))^T \tag{22}$$

where $S_{\underline{v}\underline{v}}(\underline{z})$, $S_{\underline{r}\underline{r}}(\underline{z})$ are PSD matrices of subband $\underline{v}(\underline{n})$ and random error $\underline{r}(\underline{n})$ respectively. Then we can expand the multidimensional polyphase matrices $\mathcal{H}_p(\underline{z})$, $\mathcal{G}_p(\underline{z})$ in terms of matrix polynomials such that

$$\mathcal{H}_p(\underline{z}) = \sum_{\underline{n} \in \Lambda} \mathcal{H}_{p,\underline{n}} \underline{z}^{-\underline{n}}, \quad \mathcal{G}_p(\underline{z}) = \sum_{\underline{n} \in \Lambda} \mathcal{G}_{p,\underline{n}} \underline{z}^{-\underline{n}} \tag{23}$$

where the $M \times M$ analysis/synthesis polyphase coefficient matrices are

$$\mathcal{H}_{p,\underline{n}} = \begin{bmatrix} h_0(D\underline{n}+\underline{k}_0) & h_0(D\underline{n}+\underline{k}_1) & \cdots & h_0(D\underline{n}+\underline{k}_{M-1}) \\ h_1(D\underline{n}+\underline{k}_0) & h_1(D\underline{n}+\underline{k}_1) & \cdots & h_1(D\underline{n}+\underline{k}_{M-1}) \\ \vdots & \vdots & \ddots & \vdots \\ h_{M-1}(D\underline{n}+\underline{k}_0) & h_{M-1}(D\underline{n}+\underline{k}_1) & \cdots & h_{M-1}(D\underline{n}+\underline{k}_{M-1}) \end{bmatrix},$$

$$\mathcal{G}_{p,\underline{n}} = \begin{bmatrix} g_0(D\underline{n}-\underline{k}_0) & g_0(D\underline{n}-\underline{k}_1) & \cdots & g_0(D\underline{n}-\underline{k}_{M-1}) \\ g_1(D\underline{n}-\underline{k}_0) & g_1(D\underline{n}-\underline{k}_1) & \cdots & g_1(D\underline{n}-\underline{k}_{M-1}) \\ \vdots & \vdots & \ddots & \vdots \\ g_{M-1}(D\underline{n}-\underline{k}_0) & g_{M-1}(D\underline{n}-\underline{k}_1) & \cdots & g_{M-1}(D\underline{n}-\underline{k}_{M-1}) \end{bmatrix} \tag{24}$$

Note that the negative coset vectors $\{\underline{k}_l\}$ are used in the synthesis polyphase coefficient matrix because of the positive exponent shift vectors at the synthesis side in Fig. 4 (a). Then the correlation matrix $R_{\underline{\eta}_q\underline{\eta}_q}(k)$ can be represented as

$$R_{\underline{\eta}_q\underline{\eta}_q}(k) = \mathcal{G}_{p,-k}^T B * R_{\underline{v}\underline{v}}(\underline{k}) * B(\mathcal{G}_{p,k}^T)^T + \mathcal{G}_{p,-k}^T * R_{\underline{r}\underline{r}}(\underline{k}) * (\mathcal{G}_{p,k}^T)^T. \tag{25}$$

At $k = 0$, (25) becomes the covariance matrix

$$\begin{aligned}R_{\underline{\eta}_q\underline{\eta}_q}(\underline{0}) = &\sum_{\underline{j} \in \Lambda} \sum_{\underline{k} \in \Lambda} \mathcal{G}_{p,\underline{j}}^T B R_{\underline{v}\underline{v}}(\underline{j}-\underline{k}) B \mathcal{G}_{p,\underline{k}} \\ &+ \sum_{\underline{j} \in \Lambda} \sum_{\underline{k} \in \Lambda} \mathcal{G}_{p,\underline{j}}^T R_{\underline{r}\underline{r}}(\underline{j}-\underline{k}) \mathcal{G}_{p,\underline{k}}.\end{aligned} \tag{26}$$

From Fig. 4(b), we can demonstrate that $R_{\underline{y}\underline{y}}(\underline{0})$ is the covariance matrix of the block output vector

$$\begin{aligned}\underline{y}^T(\underline{n}) &= [\eta_0(\underline{n}), \eta_1(\underline{n}), \cdots, \eta_{M-1}(\underline{n})] \\ &= [y(D\underline{n}+\underline{k}_0), y(D\underline{n}+\underline{k}_1), \cdots, y(D\underline{n}+\underline{k}_{M-1})]\end{aligned}$$

Therefore, the MS quantization error at the reconstructed output can be defined as

$$\begin{aligned}\sigma_q^2 &= E[|\underline{y}(\underline{n}) - \underline{y}(\underline{n})|^2] = \frac{1}{M}\ \mathrm{Trace}[R_{\underline{\eta}_q\underline{\eta}_q}(0)] \\ &\triangleq \sigma_d^2 + \sigma_n^2\end{aligned} \tag{27}$$

The distortion and random components of the error are

$$\begin{aligned}\sigma_d^2 &= \frac{1}{M}\ \mathrm{Trace}\Big[\sum_{\underline{j} \in \Lambda} \sum_{\underline{k} \in \Lambda} \mathcal{G}_{p,\underline{j}}^T B R_{\underline{v}\underline{v}}(\underline{j}-\underline{k}) B \mathcal{G}_{p,\underline{k}}\Big], \\ \sigma_n^2 &= \frac{1}{M}\ \mathrm{Trace}\Big[\sum_{\underline{j} \in \Lambda} \sum_{\underline{k} \in \Lambda} \mathcal{G}_{p,\underline{j}}^T R_{\underline{r}\underline{r}}(\underline{j}-\underline{k}) \mathcal{G}_{p,\underline{k}}\Big],\end{aligned} \tag{28}$$

and $R_{\underline{v}\underline{v}}(\underline{m}) = E[\underline{v}(\underline{n})v^T(n+\underline{m})]$ and $R_{\underline{r}\underline{r}}(\underline{m}) = E[\underline{r}(\underline{n})r^T(\underline{n}+\underline{m})]$ are the correlation matrices of decimated signal $\underline{v}(\underline{n})$ and random fictitious noise $\underline{r}(n)$. Note that the summation index $\underline{j}$, $\underline{k}$ in (28) are not scalars, but N-dimensional vectors corresponding to the polyphase coefficient matrices.

In order to get a parametrized multidimensional MSE measure, we substitute the synthesis polyphase coefficient matrices into (28). Then with some mathmatical manipulation, we can show that the multidimensional version of

the distortion component of the output MSE is

$$\sigma_d^2 = \frac{1}{M} \sum_{\underline{m}} \sum_{i=0}^{M-1} \sum_{j=0}^{M-1} (\alpha_i - 1)(\alpha_j - 1) R_{v_i v_j}(\underline{m}) \sum_{\underline{l} \in \Lambda} g_i(\underline{l}) g_j(D\underline{m} + \underline{l}), \tag{29}$$

and the random component is

$$\sigma_n^2 = \frac{1}{M} \sum_{\underline{m}} \sum_{i=0}^{M-1} \sum_{j=0}^{M-1} R_{r_i r_j}(\underline{m}) \sum_{\underline{l} \in \Lambda} g_i(\underline{l}) g_j(D\underline{m} + \underline{l}) \tag{30}$$

where $\sigma_{v_i}^2 = \alpha_i \sigma_{\tilde{v}_i}^2 = \alpha_i \beta_i 2^{-2R_i} \sigma_{\tilde{v}_i}^2$.

As in 1-D case in ref[11], we assume $R_{rr}(\underline{k})$ is diagonal and white such that

$$E[r_i(\underline{n}) r_j(\underline{n} + \underline{m})] = \sigma_{v_i}^2 \delta_{i-j} \delta(\underline{m}).$$
$$R_{\underline{r}\underline{r}}(\underline{k}) = \mathrm{diag}[\sigma_{r_0}^2, \sigma_{r_1}^2, \cdots, \sigma_{r_{M-1}}^2] \tag{31}$$

Then the distortion component remains as in (29), but the random component reduces to a simple form

$$\sigma_n^2 = \frac{1}{M} \sum_{i=0}^{M-1} \sigma_{r_i}^2 \sum_{\underline{l} \in \Lambda} g_i^2(\underline{l}) \tag{32}$$

so that the total mean square(MS) quantization error is just the sum of (29) and (32).

From Fig. 4(a), the correlation function $R_{v_i v_j}(\underline{m})$ in (29) can be represented as

$$R_{r_i r_j}(\underline{m}) = E[v_i(\underline{n}) v_j(\underline{n} + \underline{m})]$$
$$= E[x_i(D\underline{n}) x_j(D(\underline{n} + \underline{m}))] = R_{x_i x_j}(D\underline{m}). \tag{33}$$

Furthermore, we can express the subband correlation function $R_{x_i x_j}(\underline{m})$ in terms of the input correlation and the analysis filter impulse responses such that

$$R_{x_i x_j}(\underline{m}) = R_{xx}(\underline{m}) * h_i(\underline{m}) * h_j(-\underline{m})$$
$$= \sum_k \Big(\sum_l h_i(k + l) h_j(l) \Big) R_{xx}(\underline{m} - \underline{k}). \tag{34}$$

Thus we have formulated the N dimensional output MSE explicitly in terms of the analysis/synthesis filter coefficients, the subsampling lattice, the input signal correlation model, and implicitly in terms of the bit allocation for each band. Our objective is to find the optimal PR filter bank which minimizes this MSE for a given total bit allocation. Note that the MS quantization error formula in (29) and (32) depends on the choice of sampling matrix D rather than a scalar M as in 1-D case.

Ⅳ. Optimum Design for 2D Nonseparable Orthonormal Filter Bank

In this section, we will first consider 2D perfect reconstruction conditions for the orthonormal filter bank as a generalization of the 1-D version. Then we will develop the optimum nonseparable 2D orthonormal filter bank structure with quincunx sampling matrix.

A. 2D Nonseparable Orthonormal Subband Filter Bank

Orthonormal filter banks satisfy PR when the synthesis polyphase matrix satisfies[5][6][14]

$$\mathcal{G}_p(z) = \underline{z}^{-\underline{l}} \mathcal{H}_p(z^{-I}) J, \tag{35}$$

from the sufficient PR condition

$$\mathcal{P}(\underline{z}) = \mathcal{G}_p^T(\underline{z}) \mathcal{H}_p(\underline{z}) = \underline{z}^{-\underline{l}} I. \tag{36}$$

For this case, the analysis/synthesis polyphase matrices are lossless such that

$$\tilde{\mathcal{H}}_p(\underline{z}) \mathcal{H}_p(\underline{z}) = I, \quad \text{and} \quad \tilde{\mathcal{G}}_p(\underline{z}) \mathcal{G}_p(\underline{z}) = I. \tag{37}$$

where $\tilde{\mathcal{H}}_p(\underline{z}) \triangleq \mathcal{H}_p^*(\underline{z}^{-I})$. In the spatial-domain, this condition becomes

$$\rho_{rs}(D\underline{n}) = < h_r(\underline{k}), h_s(D\underline{n} + \underline{k}) > = \delta_{rs} \delta(\underline{n}), \tag{38}$$

which implies the following orthonormality conditions

$$\sum_{\underline{k} \in \Lambda} h_r(\underline{k}) h_r(D\underline{n} + \underline{k}) = \delta(n), \quad \sum_{\underline{k} \in \Lambda} h_r(\underline{k}) h_s(D\underline{n} + \underline{k}) = 0$$
$$\text{for } r \neq s. \tag{39}$$

Eq. (39) states that each filter $\{h_r(\underline{k})\}$ is orthogonal to its translate $h_s(D\underline{n} + \underline{k})$ and $\{h_r(\underline{k})\}$ is orthogonal to $\{h_s(\underline{k})\}$ and to all translation in lattice of $\{h_s(\underline{k})\}$. This is a lattice extension of orthonormal PR condition[5].

For the 2D two-channel orthonormal filter bank with $H_0(z_1, z_2)$ of size $L_1 \times L_2$(=even) FIR filter, we choose

$$H_1(z_1, z_2) = z_1^{-(L_1-1)} z_2^{-(L_2-1)} H_0(-z_1^{-1}, -z_2^{-1})$$
$$\Leftrightarrow h_1(n_1, n_2) = (-1)^{(n_1+n_2+1)} h_0(L_1 - 1 - n_1, L_2 - 1 - n_2) \tag{40}$$

to satisfy orthonormal PR conditions. Then the synthesis filters are spatially reversed versions of the analysis filters [6][14]

$$G_0(z_1, z_2) = z_1^{-(L_1-1)} z_2^{-(L_2-1)} H_0(z_1^{-1}, z_2^{-1})$$
$$\Leftrightarrow g_0(n_1, n_2) = h_0(L_1 - 1 - n_1, L_2 - 1 - n_2),$$

$$G_1(z_1, z_2) = z_1^{-(L_1-1)} z_2^{-(L_2-1)} H_1(z_1^{-1}, z_2^{-1})$$
$$\Leftrightarrow g_1(n_1, n_2) = h_1(L_1-1-n_1, L_2-1-n_2)$$
$$= (-1)^{(n_1+n_2)} h_0(n_1, n_2). \quad (41)$$

From Eq. (37), we can rewrite the orthonormal PR condition in (39) in terms of synthesis filters. Then the orthonormality conditions removes the cross-correlation effects between the channels in output MSE expression in (29) and (32). Thus the 2D version of MS quantization error formula reduces to

$$\sigma_{y_s}^2 = \sigma_d^2 + \sigma_n^2$$

$$\sigma_d^2 = \frac{1}{M} \sum_{i=0}^{M-1} (\alpha_i s_i - 1)^2 \sigma_{v_i}^2, \quad \sigma_n^2 = \frac{1}{M} \sum_{i=0}^{M-1} s_i^2 \sigma_{v_i}^2 \quad (42)$$

where $\sigma_{v_i}^2 = \sum_k \sum_l h_i(k) h_i(l) R_{xx}(k-l)$.

B. Optimum Design Example for 2D Nonseparable Orthonormal Suband Structure

Design example for the optimum nonseparable orthonormal filter bank is presented for 2D two-channel filter bank with equal size 4×3 filters.

The optimization algorithm is based on the exhaustive search of all possible bit allocations constrained by the total number of bits. For each bit combinations, we compute the optimal filter coefficients, and the associated MSE. We choose the one with the smallest MSE among them.

The tested input image is the standard 256×256 LENA. Thus we will show the analysis and simulation results of the designed optimal filters based on the LENA image.

We assume globally stationary source model for the test images which is a rather strong assumption, but it makes the analysis simpler. Then the separable autocorrelation function of AR(1) source can be written as

$$R_{xx}(m, n) = \sigma_x^2 \rho_h^{|m|} \rho_v^{|n|} \quad (43)$$

where the input variance $\sigma_x^2 = \dfrac{1}{(1-\rho_h^2)(1-\rho_v^2)}$, and ρ_h, ρ_v are directional correlation coefficients. Note that the first-order correlation coefficients ρ_h, ρ_v can be easily determined from

$$\rho_h = R_{xx}(1, 0), \quad \rho_v = R_{xx}(0, 1) \quad (44)$$

with respect to normalized input variance $\sigma_x^2 = 1$. This pair of parameters for LENA image is known to be $\rho_h = 0.942$ and $\rho_v = 0.972$[6].

To calculate the quantization error variance $\sigma_{v_i}^2$ in (29), we actually simulate the parameter β_i by using

$$\sigma_{v_i}^2 = \beta_i 2^{-2R_i} \sigma_{y_i}^2, \quad (45)$$

with the bits allocated to the Lloyd-Max quantizer. These are shown in Fig. 5 for LENA input image.

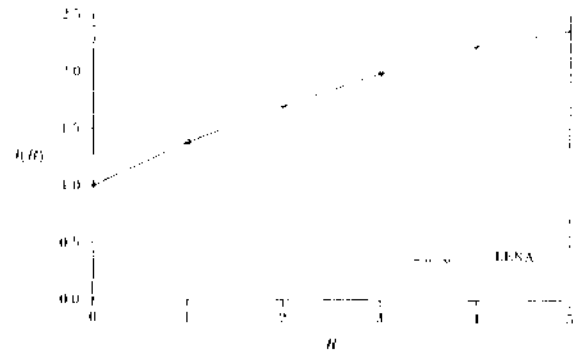

Fig. 5 $\beta(R)$ vs. R for AR(1) gaussian LENA input image

The optimal design for the nonseparable orthonormal FB is shown in table I for input testing image. The corresponding optimal impulse responses for testing image is given in table II.

Table I. Bit allocations and simulated MSE for optimum nonseparable orthonormal FB

R	R_0	R_1	MSE
1	1	1	0.3243
1.5	2	1	0.0925
2	3	1	0.0382

Table II Optimal filter coefficients of LPF $h_0(n_1, n_2)$ for nonseparable orthonormal FB

$\downarrow n_1, \rightarrow n_2$	0	1	2
(a)		$R = 1$ bits/pixel	
0	-1.478e-31	-0.21326	4.283e-34
1	0.73279	0.53332	6.525e-02
2	0.29306	0.11875	-0.16320
3	-4.067e-34	4.747e-02	-3.408e-32
		$R = 1.5$ bits/pixel	
0	1.772e-22	-0.21404	5.578e-33
1	0.73124	0.53220	6.728e-02
2	0.29409	0.12175	-0.16729
3	-3.950e-33	4.897-02	4.055e-23
		$R = 2$ bits/pixel	
0	-3.167e-21	-0.21405	1.385e-32
1	0.73123	0.53218	6.730e-02
2	0.29411	0.12177	-0.16732
3	-3.218e-32	4.898e-02	-7.248e-22

As we see from Table I, the output MSE tend to decrease as the average bit rate R is increased. We also note

the significance of the optimal bit allocations at the low frequency side of subband image. This is because the most energy of the input testing image resides in the lower frequencies than high frequencies. From Table II, we see the insensitivity of the orthonormal FB to changes in average bit rate R although the output MSE is highly dependent on them. Therefore it provides a robust system to changes in input image statistics.

Fig. 6 shows the simulation results of the total output MSE with distortion component σ_d^2 and random component σ_n^2. It demonstrates that the random component is a dominant error source in the output MSE.

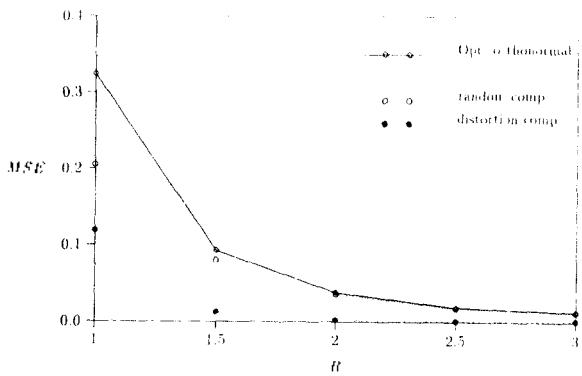

Fig. 6 The output MSE comparison of designed optimum orthonormal FB with distortion and random component of error.

V. Conclusions

We have presented a methodology for the modelling, analysis and design of the optimum nonseparable filter bank in the presence of quantization noise in multidimensional M-band subband filter banks. The optimized structure consists of optimum filter coefficients, bit allocation and pdf-optimized quantizer with PR constraints imposed on the non-quantized codec.

We have designed the optimum orthonormal FB for the nonseparable case and tested optimum design on the standard LENA image. From the simulation results, we observed two importatant facts about the designed optimum system. First, the optimally designed orthonormal subband system provides the robustness to the variations of input statistics. In orther words, whatever the input image is, we might still use a fixed designed filters because of the robustness of the filter. Second, the random component of error dominates in the total output MSE. This indicates the possible reduction of total ouptut MSE by monitoring the random component of error in proper way. Yet this topic is under investigation.

Finally, we emphasize that our approach is so general to apply the system of any dimensionality and any subsampling matrices.

References

1. E. Viscito and J. P. Allebach, "The analysis and design of multidimensional FIR perfect reconstruction filter banks for arbitrary sampling lattices," *IEEE Trans. Circuits Syst.*, vol. CAS-38, no. 1, pp. 29-41, Jan. 1991.
2. M. Vetterli, "Multidimensional subband coding: Some theory and algorithms," *Signal Processing*, vol. 6, no. 2, pp. 97-112, Feb. 1984.
3. J. W. Woods and S. O'Neil, "Subband coding of images," *IEEE Trans. Acoust., Speech, Signal Processing*, vol. 34, no. 5, pp. 421-428, Oct. 1986.
4. G. Karlsson and M. Vetterli, "Theory of two-dimensional multirate filter banks," *IEEE Trans. Acoust. Speech, Signal Processing*, vol. 38, no. 6, pp. 925-937, June 1990.
5. J. Kovačević and M. Vetterli, "Nonseparable multidimensional perfect reconstruction filter banks and wavelet bases for R^n," *IEEE Trans. Information Theory*, vol. 38, no. 2, pp. 533-555, Mar. 1992.
6. A. N. Akansu and R. A. Haddad, *Multiresolution Signal Decomposition: Transforms, Subbands, and Wavelets*. Academic Press, 1992.
7. P. H. Westerink, D. E. Boekee, J. Biemond, and J. W. Woods "Subband coding images using vector quantization," *IEEE Trans. Comm.*, vol. 36, no. 6, June 1988.
8. P. H. Westerink, J. Biemond, D. E. Boekee, "Scalar quantization error analysis for image subband coding using QMF's," *IEEE Trans. Signal Processing*, vol. 40, no. 2, pp. 421-428, Feb. 1992.
9. L. Vandendorpe, "Optimized quantization for image subband coding," *Signal Processing, Image Communication, Elsevier, Amserdam*, vol. 4, no. 1, pp. 65-80, Nov. 1991.
10. N. S. Jayant and P. Noll, *Digital Coding of Waveforms*. Englewood Cliffs, NJ: Prentice-Hall, 1984.
11. R. A. Haddad and Kyusik Park, "Modeling, analysis and optimum design of quantized M-band filter banks," *IEEE Trans. Signal Processing*, Oct. 1996.
12. S. P. Lloyd, "Least squares quantization in PCM," *Inst. of Mathematical Sciences Meeting*, Atlantic City, NJ, Sept. 1957.
13. J. Max, "Quantizing for minimum distortion," *IRE Trans. Info. Theory*, vol. IT-6, pp. 7-12, Mar. 1960.
14. P. P. Vaidyanathan, *Multirate Systems and Filter Banks*. Englewood Cliffs, NJ: Prentice-Hall, 1993.

▲Kyusik Park

Kyusik Park received B.S, M.S, and Ph.D degrees in 1986, and 1994, respectively, all from the Department of Electrical Engineering of Polytechnic University, Brooklyn, NY, USA.

In 1994, he joined the Semiconductor Division of Samsung Electronics as a staff engineer. He is currently an assistant professor with the Department of Information and Telecommunication in Sangmyung University, Chungchongnam-Do, Korea. His research interests are digital signal and image processing, and digital communication.

▲Won Cheol Lee

Won Cheol Lee was born on December 26, 1963, in Seoul, Korea. He received B.S. degree in electronics engineering from Sogang University, Seoul, Korea in 1986, the M.S. degree in electronics engineering from Yonsei University, Seoul, Korea in 1988 and the Ph.D. degree in electrical engineering from Polytechinc University, Brooklyn, New York, in 1994.

From January 1991 to July 1995, he held teaching and research fellow, and served as a postdoctoral researcher at Polytechnic University. In 1995, he joined the faculty of Soongsil University, Seoul, Korea., as an Assistant professor of the Department of Information and Telecommunication. His current research interests are digital signal processing, spectrum estimation and wireless communication.